VOLUME 117, NUMBER 5
FEBRUARY 8, 1995

JOURNAL
OF THE
AMERICAN
CHEMICAL
SOCIETY

Kinetics and Mechanism of the Oxidation of Sugars and Nucleotides by Oxoruthenium(IV): Model Studies for Predicting Cleavage Patterns in Polymeric DNA and RNA

Gregory A. Neyhart, Chien-Chung Cheng, and H. Holden Thorp*

Contribution from the Department of Chemistry, University of North Carolina, Chapel Hill, North Carolina 27599-3290

Received October 14, 1994[⊗]

Abstract: Kinetic parameters for the oxidation of D-ribose, 2-deoxy-D-ribose, adenosine 5′-monophosphate (AMP), adenosine 5′-diphosphate (ADP), 2′-deoxyadenosine 5′-monophosphate (dAMP), cytidine 5′-monophosphate (CMP), 2′-deoxycytidine 5′-monophosphate (dCMP), and thymidine 5′-monophosphate (TMP) by $Ru(tpy)(bpy)O^{2+}$ were determined in pH 7 phosphate buffer (tpy = 2,2′,2″-terpyridine, bpy = 2,2′-bipyridine). Plots of k_{obs} vs [substrate] were linear for the oxidation of ribose, 2-deoxyribose, TMP, and dCMP, yielding second-order rate constants of 0.029, 0.082, 0.38, and 0.46 M^{-1} s^{-1}, respectively. From the temperature dependence of the rate constant, activation parameters consistent with the oxidation of other organic molecules by hydride transfer were found. For CMP, AMP, and dAMP, k_{obs} vs [substrate] plots were curved due to electrostatic binding of $Ru(tpy)(bpy)O^{2+}$ to the dianionic nucleotides, and the data were treated using double-reciprocal plots, yielding effective second-order rate constants of 0.10, 0.39, and 2.5 M^{-1} s^{-1}, respectively. Product analysis by HPLC shows that a quantitative yield of free cytosine is obtained upon oxidation of dCMP based on nucleotide consumed. In TMP oxidations, an 80% yield of free thymine is observed based on $Ru(tpy)(bpy)O^{2+}$ consumed. The kinetics and product analyses are consistent with sugar oxidation at the 1′ position, and the increased reactivity of DNA compared to RNA can be understood on the basis of deactivation of the sugar oxidation product by the polar effect of the 2′-hydroxyl. The oxidation of the guanine base in GMP by $Ru(tpy)(bpy)O^{2+}$ proceeds via an oxo transfer mechanism where the initial step is formation of a bound $Ru^{III}OR^{2+}$ intermediate. The ratio of the rate-determining rate constant for oxidation of guanine nucleotides to the average rate constant of sugar oxidation predicts the relative yields of base and sugar oxidation on sequencing gels.

There has been a great deal of recent interest in the mechanisms of DNA cleavage as viewed in a kinetic context.[1-4] The goal of these studies has been to uncover the rate-determining step to understand which stage in the reaction determines the selectivity in the cleavage pattern discerned on high-resolution sequencing gels. In general, these studies have relied on the analyses of DNA products by electrophoresis or HPLC. These methods provide information on the net reaction, but the precise sequence of events must be determined by inference based on product yields. We have sought to develop a system wherein these studies could be complemented by real-time kinetic information obtained from optical spectroscopy of the cleavage agent.

The complex $Ru(tpy)(bpy)O^{2+}$ oxidizes organic substrates by hydride abstraction or oxo transfer (tpy = 2,2′,2″-terpyridine,

[⊗] Abstract published in *Advance ACS Abstracts*, January 15, 1995.

(1) Van Atta, R. B.; Long, E. C.; Hecht, S. M.; van der Marel, G. A.; van Boom, J. H. *J. Am. Chem. Soc.* **1989**, *111*, 2722.
(2) Myers, A. G.; Cohen, S. B.; Kwon, B. M. *J. Am. Chem. Soc.* **1994**, *116*, 1670–1682.
(3) Myers, A. G.; Cohen, S. B.; Kwon, B. M. *J. Am. Chem. Soc.* **1994**, *116*, 1255–1271.
(4) Worth, J. L.; Frank, B. L.; Christner, D. F.; Absalon, M. J.; Stubbe, J.; Kozarich, J. W. *Biochemistry* **1993**, *32*, 2601.

0002-7863/95/1517-1463$09.00/0

Scheme 1

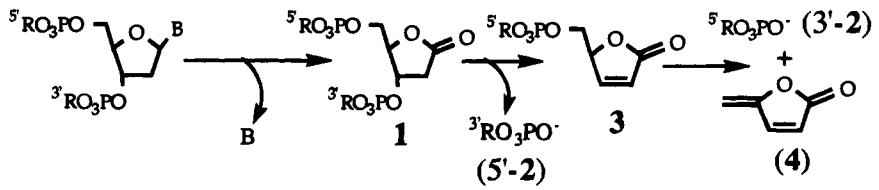

bpy = 2,2′-bipyridine).[5,6] We have shown that this complex and its derivatives cleave DNA by sugar oxidation at the 1′ position and oxidation of guanine.[7-11] Oxidation at the 1′ position leads to release of free bases and a furanone product,[12] as shown in Scheme 1. We have shown that the guanine oxidation pathway provides more cleavage on sequencing gels than the sugar pathway following piperidine treatment with a 3:2 ratio of total guanine oxidation to total sugar oxidation. We report here on kinetic studies of the oxidation of model nucleotides and sugars aimed at understanding this observation on the basis of the relative reactivities of the oxidized functionalities.

There has been considerable interest in understanding the differences in reactivity of DNA and RNA. Holmes and Hecht have shown that iron bleomycin (FeBLM) cleaves a particular tRNA and an analogous tDNA at the same site.[13] Upon increasing the concentration of FeBLM, additional cleavage sites are observed in tDNA but not tRNA, suggesting that the general reactivity of DNA is higher than that of RNA. Lim and Barton have made related observations on the photooxidation of analogous DNA and RNA polymers with complexes based on $Rh(phen)_2(phi)^{3+}$ (phen = 1,10-phenanthroline, phi = phenanthrenequinone diimine), reporting 17 cleavage sites for tDNA and only 7 for tRNA.[14] We report here that $Ru(tpy)(bpy)O^{2+}$ is also more reactive toward DNA than an analogous RNA, and this result is consistent with kinetic studies on mononucleotides.

Experimental Section

Materials. D-Ribose was obtained from Fluka Chemika-Bio-Chemika and used as received. 2-Deoxy-D-ribose, adenosine 5′-monophosphate·$2.5H_2O$, sodium salt; adenosine 5′-diphosphate·$1.5H_2O$, potassium salt; 2′-deoxyadenosine 5′-monophosphate·$4H_2O$, disodium salt; cytidine 5′-monophosphate·$6H_2O$, disodium salt; 2′-deoxycytidine 5′-monophosphate·$2.5H_2O$, disodium salt; guanosine 5′-monophosphate·$6.5H_2O$, disodium salt; and thymidine 5′-monophosphate·H_2O, disodium salt were obtained from Sigma Chemical Co. and used as received. pH 7 phosphate buffer solutions were made using $NaH_2PO_4·H_2O$ and $Na_2HPO_4·7H_2O$ obtained from Fisher Scientific and house distilled water which was further purified by passage through a Millipore Milli-Q water purification system. The complex $[Ru(tpy)(bpy)O](ClO_4)_2$ was prepared by literature methods.[21]

Measurements. Absorbance vs time data were collected on a Cary 14 spectrophotometer modified by On Line Instrument Systems (OLIS). Aliquots of stock substrate solutions were added to solutions of oxoruthenium(IV) and mixed by hand in the cuvette. The temperature was controlled using a Fisher Isotemp Model 910 circulating bath. The data were fit to exponentials using the OLIS nonlinear least-squares fitting routines. Rate constants were analyzed using KaleidaGraph software.

HPLC analyses were carried out using a Millipore system comprised of a Waters Model 510 pump, Model 717 autosampler, and Model 996 photodiode array detector. The system was controlled and the data analyzed using the Millennium software package. Analytical separations were accomplished on a Rainin Microsorb-MV reverse phase C-18 column (4.6 × 100 mm, 3 μm particle size). Elution conditions are given in the text and figure legends.

Kinetics experiments for guanine nucleotides were carried out using an OLIS-RSM stopped-flow apparatus equipped with a rapid scanning monochromator. Solutions were maintained at 25 ± 1 °C. The instrument has a time resolution of 1 scan per millisecond, although for these reactions (10−60 s), an averaging mode producing 31 scans per second was used. The data were transferred for kinetic analysis to the SPECFIT software package, provided Dr. Robert A. Binstead of Spectrum Software Associates, Chapel Hill, NC. SPECFIT is a global least-squares fitting routine for equilibrium and kinetic studies, which uses factor analysis and Marquardt minimization.

Hairpin Oxidation. The DNA purification, ^{32}P-labeling, and sequencing gels were performed as described previously.[7] Formation of the hairpin structure was accomplished by heating the DNA solution at 60 °C for 5 min and then slowly cooling to room temperature over a 3−5 h period. The denatured DNA was prepared by heating as described above and rapidly cooling to 0°C in an ice bath. Cleavage of the denatured DNA by $Ru(tpy)(bpy)O^{2+}$ produced a significantly different cleavage pattern than cleavage of the hairpin, indicating that the proper hairpin structure was formed by slow cooling.

Results

Oxidation of DNA and organic molecules in aqueous solution by $Ru(tpy)(bpy)O^{2+}$ proceeds in two stages.[5,15] In the first stage, $Ru(tpy)(bpy)O^{2+}$ is reduced via hydride transfer followed by protonation to form $Ru(tpy)(bpy)OH_2^{2+}$:

$$Ru^{IV}(tpy)(bpy)O^{2+} + RH \rightarrow R^+ + Ru^{II}(tpy)(bpy)OH^+ \quad (1)$$

$$Ru^{II}(tpy)(bpy)OH^+ + H^+ \rightarrow Ru^{II}(tpy)(bpy)OH_2^{2+} \quad (2)$$

Once $Ru(tpy)(bpy)OH_2^{2+}$ is generated, comproportionation with $Ru(tpy)(bpy)O^{2+}$ occurs to generate $Ru(tpy)(bpy)OH^{2+}$:

$$Ru^{IV}(tpy)(bpy)O^{2+} + Ru^{II}(tpy)(bpy)OH_2^{2+} \rightarrow 2\,Ru^{III}(tpy)(bpy)OH^{2+} \quad (3)$$

Thus, the net effect of the first stage is to convert all of the $Ru(tpy)(bpy)O^{2+}$ into $Ru(tpy)(bpy)OH^{2+}$, but only half of the oxidizing equivalents end up in substrate oxidation. The second stage is three orders of magnitude slower and involves the oxidation of substrate via hydrogen atom transfer, converting $Ru(tpy)(bpy)OH^{2+}$ into $Ru(tpy)(bpy)OH_2^{2+}$:

$$Ru^{III}(tpy)(bpy)OH^{2+} + RH \rightarrow Ru^{II}(tpy)(bpy)OH_2^{2+} + R^\bullet \quad (4)$$

The $Ru^{III}OH^{2+}$ oxidant can also access the hydride abstraction

(5) Thompson, M. S.; Meyer, T. J. *J. Am. Chem. Soc.* **1982**, *104*, 4106.
(6) Dobson, J. C.; Seok, W. K.; Meyer, T. J. *Inorg. Chem.* **1986**, *25*, 1513−1514.
(7) Cheng, C.-C.; Goll, J. G.; Neyhart, G. A.; Welch, T. W.; Singh, P.; Thorp, H. H. *J. Am. Chem. Soc.*, in press.
(8) Grover, N.; Thorp, H. H. *J. Am. Chem. Soc.* **1991**, *113*, 7030.
(9) Grover, N.; Gupta, N.; Singh, P.; Thorp, H. H. *Inorg. Chem.* **1992**, *31*, 2014.
(10) Neyhart, G. A.; Grover, N.; Smith, S. R.; Kalsbeck, W. A.; Fairley, T. A.; Cory, M.; Thorp, H. H. *J. Am. Chem. Soc.* **1993**, *115*, 4423.
(11) Welch, T. W.; Neyhart, G. A.; Goll, J. G.; Ciftan, S. A.; Thorp, H. H. *J. Am. Chem. Soc.* **1993**, *115*, 9311−9312.
(12) Goyne, T. E.; Sigman, D. S. *J. Am. Chem. Soc.* **1987**, *109*, 2846.
(13) Holmes, C. E.; Hecht, S. M. *J. Mol. Biol.* **1993**, *268*, 25909−25913.
(14) Lim, A. C.; Barton, J. K. *Biochemistry* **1993**, *32*, 11029−11034.
(15) Thompson, M. S.; Meyer, T. J. *J. Am. Chem. Soc.* **1982**, *104*, 5070.

Table 1. Kinetic Parameters for the Oxidation of Sugars and Deoxypyrimidine Nucleotides by Ru(tpy)(bpy)O^{2+} in 50 mM pH 7 Phosphate Buffer Solution

substrate	$k(M^{-1}\ s^{-1})^a$	$\Delta H^{\ddagger}$ (kcal/mol)	$\Delta S^{\ddagger}$ (cal/(K·mol))
ribose	0.029	12.8	−23
deoxyribose	0.082	9.8	−39
TMP	0.39	9.9	−27
dCMP	0.46	8.5	−31

^{a} $T = 25 \pm 1$ °C.

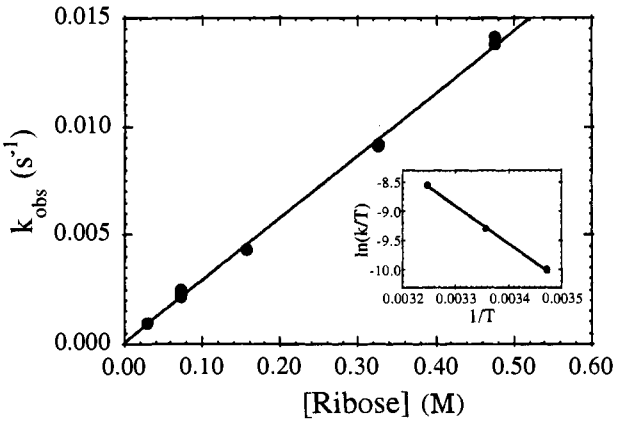

Figure 1. Plot of k_{obs} vs ribose concentration for the oxidation of ribose by 8 × 10^{-5} M Ru(tpy)(bpy)O^{2+} in 50 mM pH 7 phosphate buffer solution. Inset: Temperature dependence of the second-order rate constant where [ribose] = 0.157 M and [Ru] = 8 × 10^{-5} M.

pathway through the unfavorable disproportionation (reverse of eq 3) to $Ru^{IV}O^{2+}$. The absorption spectra of Ru(tpy)(bpy)OH_2^{2+} and Ru(tpy)(bpy)OH^{2+} exhibit an isosbestic point at 406 nm, so when the reaction is monitored at this wavelength, only the reduction of Ru(tpy)(bpy)O^{2+} is observed.[5,15] Decay curves measured at 406 nm during substrate oxidation are therefore monoexponential, and the fitted decay constants can be used directly to obtain psuedo-first-order rate constants for eq 1.

Model Sugars. The kinetics of oxidation of D-ribose and 2-deoxy-D-ribose by Ru(tpy)(bpy)O^{2+} were measured in 50 mM phosphate pH 7.1 buffer solution. The kinetics were followed by monitoring the absorbance at 406 nm versus time, which directly gives the disappearance of Ru(tpy)(bpy)O^{2+}. The reactions were run under pseudo-first-order conditions with metal complex concentrations in the range of 75−400 μM and sugar concentration in 200−6000-fold excess.

The reactions are first order in both metal complex and sugar. Absorbance vs time traces can be fit to a single-exponential function, and plots of k_{obs} vs [sugar] are linear. The second-order rate constants derived from the slopes are listed in Table 1, and representative data for ribose are plotted in Figure 1. Plots of log(k_{obs}) vs log([sugar]) are linear with slopes of 0.94 and 1.00 for the oxy and 2-deoxy forms, respectively. At constant sugar concentration, the rate constant is independent of metal concentration, as expected for a psuedo-first-order reaction. The temperature dependence of the second-order rate constant for ribose oxidation over the temperature range 15−35 °C is shown in the inset in Figure 1. Activation parameters derived from the temperature dependence are also listed in Table 1. The overall activation parameters are consistent with a hydride transfer reaction.[5,15] The 2-deoxy form of ribose is oxidized at a rate 2.5 times greater than the oxy form, and this difference in rate is apparent in the enthalpy of activation. We are interested in this point because of recent observations that RNA is apparently less reactive than DNA toward many cleavage agents.[13,14]

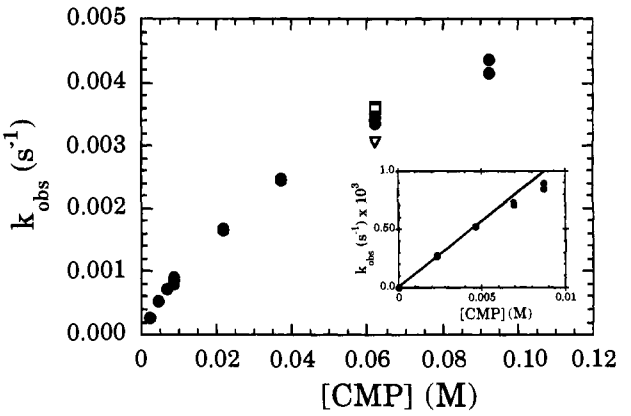

Figure 2. Plot of k_{obs} vs CMP concentration for the oxidation of CMP by 8 x 10^{-5} M Ru(tpy)(bpy)O^{2+} in 50 mM (closed circles), 15 mM (open squares), and 500 mM (open triangles) pH 7 phosphate buffer solution. Inset: Enlargement of the low [CMP] regime.

Deoxypyrimidine Nucleotides. Plots of k_{obs} vs [substrate] were linear in the [substrate] range 0−0.025 M for the oxidation of the deoxypyrimidine nucleotides 2′-deoxythymidine 5′-monophosphate (TMP)[16] and 2′-deoxycytidine 5′-monophosphate (dCMP). The second-order rate constants for the oxidation are shown in Table 1. Plots of log(k_{obs}) vs log([substrate]) had slopes only slightly less than 1 (0.86 for TMP and 0.92 for dCMP). The rate constant for oxidation of 0.022 M solutions of TMP showed a small 5% increase upon increasing the ruthenium concentration from 70 to 460 μM. The oxidation of 0.017 M solutions of dCMP showed no dependence on ruthenium concentration in the range 80−475 μM. Activation parameters derived from the temperature dependence of the rate constant in the range 15−35 °C are also shown in Table 1.

For the oxidation of cytidine 5′-monophosphate (CMP) by Ru(tpy)(bpy)O^{2+}, the plot of k_{obs} vs [CMP] shown in Figure 2 deviates significantly from linearity in the CMP concentration range 0−0.1 M. The inset shows the linear region observed at low concentrations of CMP. Using the two lowest concentrations and the origin, a second-order rate constant of 0.11 M^{-1} s^{-1} can be estimated. The rate constant for oxidation of 0.062 M CMP does appear to have a dependence on the concentration of oxoruthenium(IV). Upon increasing ruthenium concentration from 80 to 450 μM, the observed rate constant increases 25%.

We suspected that since the oxidant is a dication and CMP is a dianion, weak electrostatic binding of the reactants could introduce a rapid preequilibrium into the reaction mechanism:

$$Ru(tpy)(bpy)O^{2+} + CMP^{2-} \overset{K_b}{\rightleftharpoons} Ru(tpy)(bpy)O^{2+}\cdot CMP^{2-} \quad (5)$$

$$Ru(tpy)(bpy)O^{2+}\cdot CMP^{2-} \overset{k}{\rightarrow} Ru(tpy)(bpy)OH_2^{2+}\cdot CMP_{ox} \quad (6)$$

In this case, double-reciprocal plots of $1/k_{obs}$ vs 1/[substrate] should be linear, as shown in Figure 3. By analogy to enzyme kinetics, a value for "k_{max}" of 0.007 s^{-1} can be determined from the reciprocal of the y-intercept, and a K_b = 15 M^{-1} can be determined from the x-intercept. This small binding constant is consistent with simple electrostatic binding of a dication and dianion. The product of k_{max} and K_b gives an effective second-order rate constant of 0.10 $M^{-1}s^{-1}$, which is in good agreement with the value of 0.11 M^{-1} s^{-1} determined from the k_{obs} vs [CMP] plot (inset, Figure 2).

(16) Technically, the notation dTMP is redundant, since there is no biological oxy form of TMP.

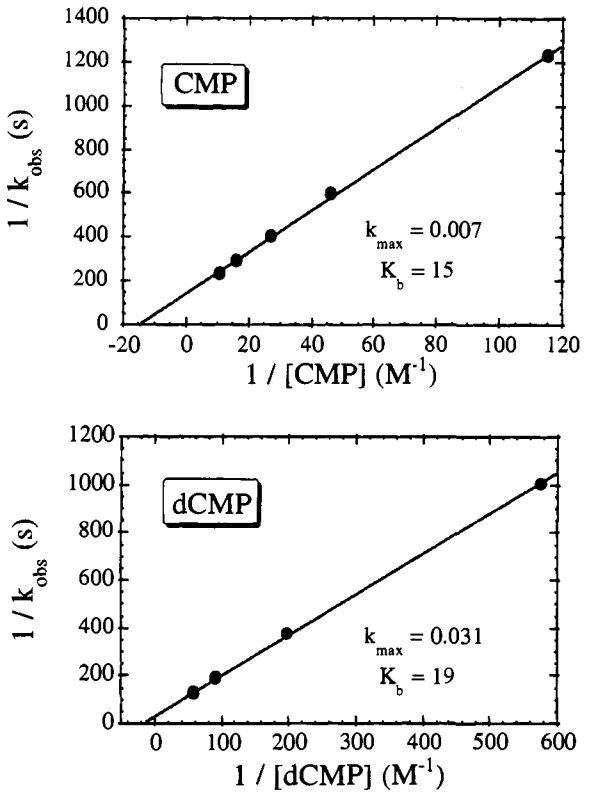

Figure 3. Double-reciprocal plot of $1/k_{obs}$ vs 1/[substrate] for the oxidation of CMP (top panel) and dCMP (bottom panel) by 8×10^{-5} M Ru(tpy)(bpy)O^{2+} in 50 mM pH 7 phosphate buffer solution.

If electrostatic interactions are responsible for the preequilibrium, the ionic strength should influence the reaction rate. To test for the effect of ionic strength on the reaction, the reaction was run with [Ru] = 8×10^{-5} M and [CMP] = 0.063 M in 15 mM (Figure 2, open squares), 50 mM (closed circles), and 500 mM (open triangles) phosphate buffer. The rate showed a small acceleration with decreasing ionic strength, as expected for a simple ion pair.[17]

Similar treatment of the dCMP oxidation data yields values of $k_{max} = 0.031\ s^{-1}$ and $K_b = 19\ M^{-1}$, and an effective second-order rate constant of 0.59 $M^{-1}\ s^{-1}$ could be calculated. This value is in fairly good agreement with that of 0.46 $M^{-1}\ s^{-1}$ determined from a plot of k_{obs} vs [dCMP] (Table 1). As with the simple sugar, oxidation of the deoxy form of the nucleotide is several times faster than oxidation of the oxy form. The reason the double-reciprocal analysis is performed for CMP is that since CMP is less reactive, higher concentrations of CMP are required to achieve similar changes in absorbance for the kinetic measurements and to ensure that psuedo-first-order conditions are still in effect. These constraints necessitate that kinetic measurements are performed in a concentration regime where significant binding occurs. Lower concentrations of dCMP can be used, so kinetic measurements can be performed over a concentration range where there is not significant binding. As will be shown below, the extent of ion pairing is similar among the different mononucleotides.

Adenine Nucleotides. Plots of k_{obs} vs [substrate] for the oxidation of adenosine 5′-monophosphate (AMP) and 2′-deoxyadenosine 5′-monophosphate (dAMP) by Ru(tpy)(bpy)-O^{2+} were also nonlinear. The nucleotide adenosine 5′-diphosphate (ADP) was also investigated, because since the diphosphate is a trianion, we expected a larger value of K_b. The

(17) Manning, G. S. *Acc. Chem. Res.* **1979**, *12*, 443.

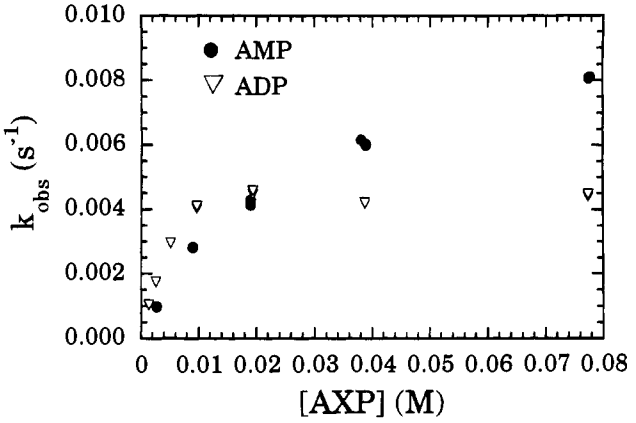

Figure 4. Plot of k_{obs} vs AXP concentration for the oxidation of AXP by 8×10^{-5} M Ru(tpy)(bpy)O^{2+} in 50 mM pH 7 phosphate buffer where AXP is AMP (closed circles) or ADP (open triangles).

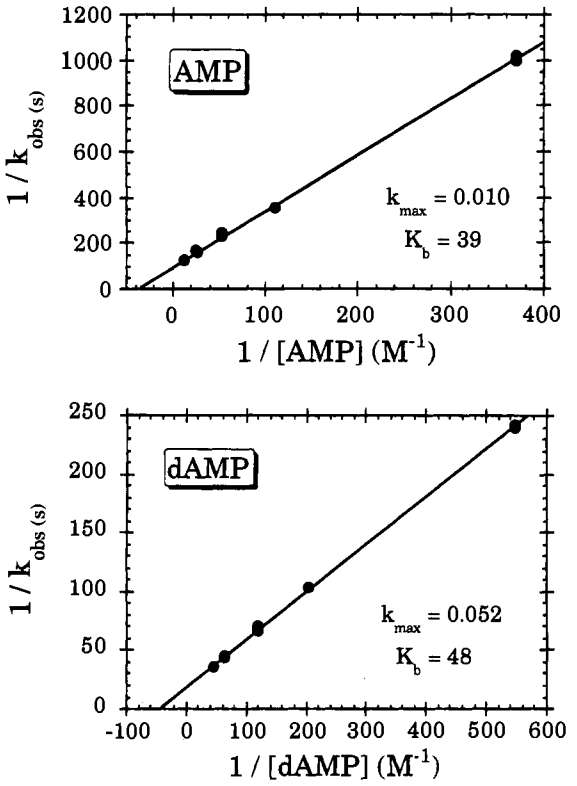

Figure 5. Double-reciprocal plot of $1/k_{obs}$ vs 1/[substrate] for the oxidation of AMP (top panel) and dAMP (bottom panel) by 8×10^{-5} M Ru(tpy)(bpy)O^{2+} in 50 mM pH 7 phosphate buffer solution.

data for AMP and ADP are shown in Figure 4. In the concentration range studied, the rate constant for the oxidation of ADP rose more steeply with concentration and reached a limiting value, as shown by the plateau in Figure 4. The rate constants for AMP and dAMP both showed some dependence on ruthenium concentration. For AMP, it increased by 23% upon increasing ruthenium from 80 to 360 μM, and for dAMP, it increased by 7% upon increasing ruthenium from 80 to 520 μM.

Double-reciprocal plots for the oxidation of AMP and dAMP are shown in Figure 5. The values determined for k_{max}, K_b, and the effective second-order rate constant for the adenine-based nucleotides are listed along with those for the cytosine-based nucleotides in Table 2. For ADP, k_{max} was taken directly from the plateau region in Figure 4. The value for K_b was determined from a double-reciprocal plot using the data from

Table 2. Kinetic Parameters for the Oxidation of Cytosine- and Adenine-Based Nucleotides by Ru(tpy)(bpy)O^{2+} at 25 ± 1 °C in 50 mM pH 7 Phosphate Buffer Solution

substrate	k_{max} (s^{-1})[a]	K_b (M^{-1})[b]	k ($M^{-1}s^{-1}$)[c]
CMP	0.0069	15	0.10
dCMP	0.031	19	0.59
AMP	0.010	39	0.39
dAMP	0.052	48	2.5
ADP	0.0043[d]	110	0.47

[a] From 1/*y*-intercept of the double-reciprocal plot, except where noted. [b] From −(*x* intercept) of the double-reciprocal plot. [c] The product of k_{max} and K_b. [d] Taken directly from the plateau region of the k_{obs} vs [ADP] plot, Figure 4.

the four lowest concentrations. Notably, the second-order rate constants calculated in this manner differed by only ~20% from AMP to ADP. As expected for an electrostatic interaction, a larger K_b was observed for the trianionic ADP nucleotide. As with the cytosine nucleotides, dAMP is oxidized by Ru(tpy)(bpy)O^{2+} about six times faster than AMP.

Model Alcohols. Since we have shown that DNA oxidation by Ru(tpy)(bpy)O^{2+} occurs via activation of the 1′-hydrogen, we suspected that the difference in reactivity of the deoxy and oxy nucleotides was a result of the deactivation of the 1′ carbocation via the polar effect of the 2′-hydroxyl.[18] As a model for this effect, the oxidations of 2-propanol and 1,2-propanediol were compared. The oxidation of 2-propanol by Ru(tpy)(bpy)O^{2+} has been reported by Thompson and Meyer to proceed with a rate constant of 0.067 M^{-1} s^{-1} at 25 °C.[5] In our hands, the oxidation of 2-propanol proceeded with a similar rate constant of 0.090 M^{-1} s^{-1}. More important, the oxidation of 1,2-propanediol by Ru(tpy)(bpy)O^{2+} under identical conditions proceeded with a rate constant of 0.016 M^{-1} s^{-1}. Thus, it appears that hydroxyl groups on the carbon adjacent to the site of activation do indeed deactivate the substrate toward oxidation by Ru(tpy)(bpy)O^{2+}.

Guanine Nucleotides. Absorbance vs time curves at 406 nm for guanosine 5′-monophosphate (GMP) are not monoexponential, as observed with the other substrates discussed here. We have observed that Ru(tpy)(bpy)O^{2+} cleaves DNA by oxidation of guanine, which must occur by a different mechanism than sugar oxidation.[7] The decay curves for GMP oxidation are sigmoidal in shape, as shown in Figure 6A. This behavior is consistent with formation of a bound, colored intermediate and eventual overoxidation of the substrate where the first step is much slower than the subsequent steps. Thus, initial oxidation of GMP produces a species that is oxidized more rapidly than GMP itself. Oxidation of *trans*-stilbene by $Ru^{IV}O^{2+}$ occurs with an initial rate-determining step corresponding to the formation of a bound epoxide complex Ru^{III}(epoxide)$^{3+}$, and other oxo-transfer reactions of $Ru^{IV}O^{2+}$ proceed via similar initial steps.[19,20] These bound complexes are then oxidized rapidly by an additional equivalent of oxidized ruthenium.

The complete spectra from 350 to 550 nm were acquired for the first minute of the reaction of Ru(tpy)(bpy)O^{2+} with GMP, and a global fit was performed to the following kinetic model:

$$Ru^{IV}O^{2+} + GMP \xrightarrow{k_1} \mathbf{I} \quad (7)$$

$$Ru^{IV}O^{2+} + \mathbf{I} \xrightarrow{k = 50000\ M^{-1}\ s^{-1}} Ru^{III}OH^{2+} + Ru^{II}OH_2{}^{2+} + P1 \quad (8)$$

$$Ru^{III}OH^{2+} + \mathbf{I} \xrightarrow{k = 50000\ M^{-1}\ s^{-1}} 2Ru^{II}OH_2{}^{2+} + P1 \quad (9)$$

$$Ru^{IV}O^{2+} + Ru^{II}OH_2{}^{2+} \underset{k = 3000\ M^{-1}\ s^{-1}}{\overset{k = 2 \times 10^5\ M^{-1}}{\rightleftharpoons}} 2Ru^{III}OH^{2+} \quad (10)$$

$$Ru^{III}OH^{2+} + P1 \xrightarrow{k = 7000\ M^{-1}\ s^{-1}} Ru^{II}OH_2{}^{2+} + P2 \quad (11)$$

$$Ru^{III}OH^{2+} + P2 \xrightarrow{k = 7000\ M^{-1}\ s^{-1}} Ru^{II}OH_2{}^{2+} + P3 \quad (12)$$

where P1, P2, and P3 are non-colored guanine oxidation products and **I** is a bound Ru^{III}−O−GMP adduct similar to the bound epoxide produced during olefin oxidation. The results of the global fitting of the complete time-dependent spectra are shown as both sample kinetic traces (Figure 6A) and the calculated spectra of the absorbing species (Figure 6B). The SPECFIT simulation produces the calculated spectra of $Ru^{IV}O^{2+}$, $Ru^{III}OH^{2+}$, and $Ru^{II}OH_2{}^{2+}$, which all agree well with the known spectra.[21] The only calculated spectrum that we do not know explicitly from independent experiments is that of **I**, but this spectrum strongly resembles the calculated spectra of complexes of Ru^{III} with bound oxidized substrates, especially bound epoxides.[19,20] The rate constants for the comproportionation equilibrium (eq 10) are known.[5]

The quality of the fit and the magnitude of k_1 are not particularly sensitive to the precise values of the rate constants for eqs 8, 9, 11, and 12, as long as these values are much greater than k_1. Specifically, the fitted value of k_1 is the same when rate constants are used in the range 1×10^4 to 9×10^4 M^{-1} s^{-1} for eqs 8 and 9 and 1000−9000 M^{-1} s^{-1} for eqs 11 and 12. The reason for this insensitivity is that the time window of the reaction has been chosen to provide the maximum amount of information on k_1, which involves the disappearance of Ru^{IV}. Reactions 8, 9, 11, and 12 all produce Ru^{II}, which is not observed until late times in the oxidation, because of the comproportionation reaction (eq 10). The determination of k_1 using this model and time window is well-defined: experiments conducted over the concentration ranges of 0.03−0.23 mM Ru(tpy)(bpy)O^{2+} and 1−33 mM GMP give $k_1 = 9 \pm 2$ M^{-1} s^{-1}. As expected, the second-order rate constant is not a function of metal or GMP concentration. These considerations have been discussed by Meyer et al. for oxidations of other substrates.[19,20]

We have shown previously that Ru(tpy)(bpy)O^{2+} cleaves DNA by oxidation of guanine as well as by sugar oxidation and that the guanine reaction is significantly more efficient.[7] The kinetic studies reported here are consistent with our DNA results, because oxidations of the A, T, and C deoxynucleotides all exhibit single-exponential kinetics with rate constants in the same range (0.4−2 M^{-1} s^{-1}), and the guanine reaction is mechanistically more complicated and more efficient. A likely site of initial oxidation is C8 to form 8-oxoguanine,[22-24] suggesting that species **I** has the structure:

Oxidation of guanine at the C8 position has received the most attention; however, Cadet et al. have recently shown that

(18) Giese, B. *Angew. Chem., Int. Ed. Engl.* **1983**, *22*, 753.
(19) Stultz, L. K.; Binstead, R. A.; Reynolds, M. S.; Meyer, T. J. *J. Am. Chem. Soc.*, in press.
(20) Dovletoglou, A.; Meyer, T. J. *J. Am. Chem. Soc.* **1994**, *116*, 215−223.
(21) Takeuchi, K. J.; Thompson, M. S.; Pipes, D. W.; Meyer, T. J. *Inorg. Chem.* **1984**, *23*, 1845.
(22) Kasai, H.; Yamgizumi, Z.; Berger, M.; Cadet, J. *J. Am. Chem. Soc.* **1992**, *114*, 9692.
(23) Pavlov, Y. I.; Minnick, D. T.; Izuta, S.; Kunkel, T. A. *Biochemistry* **1994**, *33*, 4695−4701. Dizdaroglu, M. *Biochemistry* **1985**, *24*, 4476−4481.
(24) Cadet, J.; Berger, M.; Buchko, G. W.; Joshi, P. C.; Raoul, S.; Ravanat, J.-L. *J. Am. Chem. Soc.* **1994**, *116*, 7403−7404.

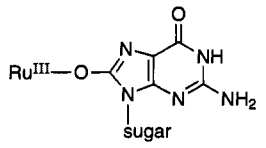

oxidation at C6 may be more important.[24,25] Partitioning of oxidation of guanine at C6 and C8 may indeed occur here. The steric demands of forming a bound intermediate at either position may have profound implications in the sequence- and structural-selectivity of guanosine oxidation[26-28] and suggest that we could control the sugar/guanine oxidation ratio by modulating the accessibility of the oxo ligand in Ru(tpy)(bpy)O^{2+}. Indeed, oxidation of DNA by Ru(tpy)(bpy)O^{2+} produces high-molecular-weight bands on sequencing gels consistent with the formation of **I** that yield scission at guanine upon piperidine treatment.[29]

Nucleotide Oxidation Products. The oxidation of nucleotides was also followed by reverse-phase HPLC analysis with diode array detection of reaction products. Reactions were run both with a large excess of nucleotide as in the kinetics experiments or with a stoichiometric amount of Ru(tpy)(bpy)-O^{2+}. Reactions were run in 100 mM ionic strength pH 7.1 phosphate buffer. Elution of products from the column was accomplished using as eluent either the buffer solution or a buffer/acetonitrile gradient (0–5 min, 0% CH_3CN; 5–40 min, 0 to 30% CH_3CN). The flow rate was maintained at 1 mL/min. No ruthenium complexes were observed using only buffer as eluent; however, a broad peak with retention time of 33–35 min and an optical spectrum similar to that of Ru(tpy)(bpy)-OH_2^{2+} was observed using the gradient elution.

The oxidation of CMP and dCMP by Ru(tpy)(bpy)O^{2+} resulted in the release of free cytosine. Stoichiometric or excess $Ru^{IV}O^{2+}$ was incubated overnight with 0.1 mM solutions of CMP or dCMP. A typical chromatogram using buffer as eluent is shown in Figure 7. A single absorbing product was observed that had a retention time and spectrum identical to that of cytosine. Comparison of integrated peak areas with those for cytosine standards shows a quantitative yield of cytosine (1.1 ± 0.1) per molecule of nucleotide consumed.

The oxidation of TMP by Ru(tpy)(bpy)O^{2+} was more complex. In reactions run in the same concentration regime as the kinetics experiments, the major reaction product was free thymine. Solutions of TMP (8 mM) containing varying concentrations of $Ru^{IV}O^{2+}$ (0.09–0.4 mM) were allowed to stand for 45 min prior to injection. This time was sufficient for all of the initial $Ru^{IV}O^{2+}$ to be consumed but short enough that there was very little contribution from the $Ru^{III}OH^{2+}$ stage of the reaction (eq 4). A typical chromatogram is shown in Figure 8a. On comparison of peak areas to thymine standards, a (40 ± 5)% yield of thymine was found based on moles of Ru(tpy)(bpy)O^{2+} consumed. Because of the comproportionation reaction (eq 3), only 50% of the $Ru^{IV}O^{2+}$ is expected to participate in substrate oxidation, so the yield of thymine is (80 ± 10)% based on the oxidant. The change in peak area of the TMP peak was sufficiently small compared to the total area so as to not provide reliable estimates of the ratio of thymine produced compared to TMP consumed.

Under conditions where a stoichiometric concentration of oxidant was used ([TMP] = 0.1 mM, [Ru(tpy)(bpy)O^{2+}] = 0.05–0.4 mM), a new peak at 1.3 min was observed (Figure 8b). Free thymine was also observed, but the yield was only 0.60 ± 0.05 per molecule of TMP consumed. Thymine is known to undergo oxidation during reactions of DNA with singlet oxygen and other radicals.[30] To test for the contribution

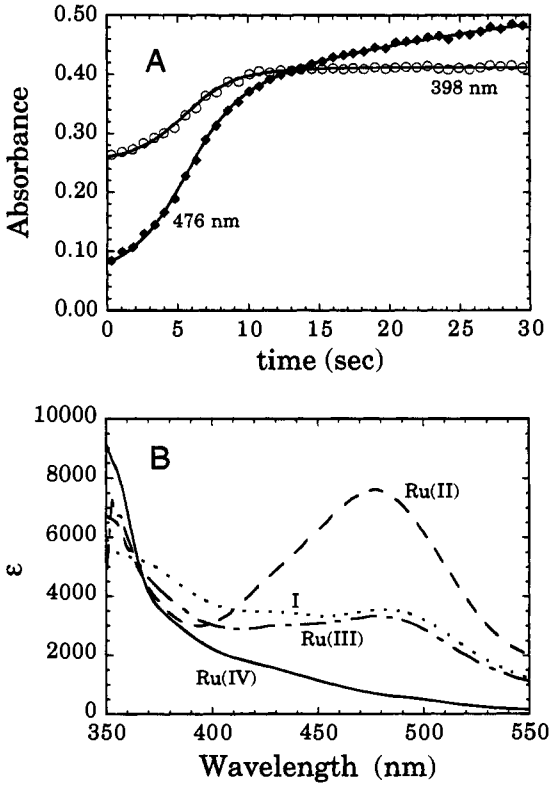

Figure 6. (A) Absorbance versus time traces at 398 nm (open circles) and 476 nm (closed diamonds) for the oxidation of GMP (3.8 mM) by Ru(tpy)(bpy)O^{2+} (0.12 mM) in 50 mM phosphate buffer (pH 7.1). Solid lines are the single-wavelength decays calculated using SPECFIT from fitting the change in the entire spectrum from 350 to 550 nm over the indicated time range. (B) Spectra calculated from the fitting procedure, see text.

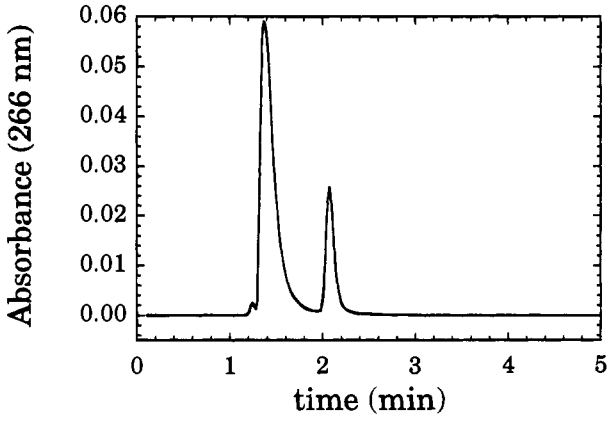

Figure 7. HPLC chromatogram at 266 nm of the reaction of 0.1 mM CMP and 0.2 mM Ru(tpy)(bpy)O^{2+} incubated overnight at 37 °C. The retention times of CMP and C are 1.4 and 2.1 min, respectively.

(25) Reaction of guanine with Ru(tpy)(bpy)O^{2+} in aqueous solution produces three products that can be readily detected by reverse-phase HPLC. One of these products has the same absorption spectrum (λ_{max} = 245, 285 nm) as 8-oxo-G and a similar retention time; however, this does not appear to be the major product. This observation could indicate that oxidation partitions between C8 and C6, as suggested by Cadet et al.,[24] or that most of the 8-oxo-G has been overoxidized, as shown in eqs 8–12. An authentic sample of 8-oxo-G was prepared according to: Cavalieri, L. F.; Bendich, A. *J. Am. Chem. Soc.* **1950**, *72*, 2587.

(26) Chen, X.; Burrows, C. J.; Rokita, S. E. *J. Am. Chem. Soc.* **1991**, *113*, 5884.

(27) Chen, X.; Burrows, C. J.; Rokita, S. E. *J. Am. Chem. Soc.* **1992**, *114*, 322.

(28) Chen, X.; Woodson, S. A.; Burrows, C. J.; Rokita, S. E. *Biochemistry* **1993**, *32*, 7610–7616.

(29) Cheng, C.-C.; Thorp, H. H. Unpublished results.

(30) Steenken, S. *Chem. Rev.* **1989**, *89*, 503–520.

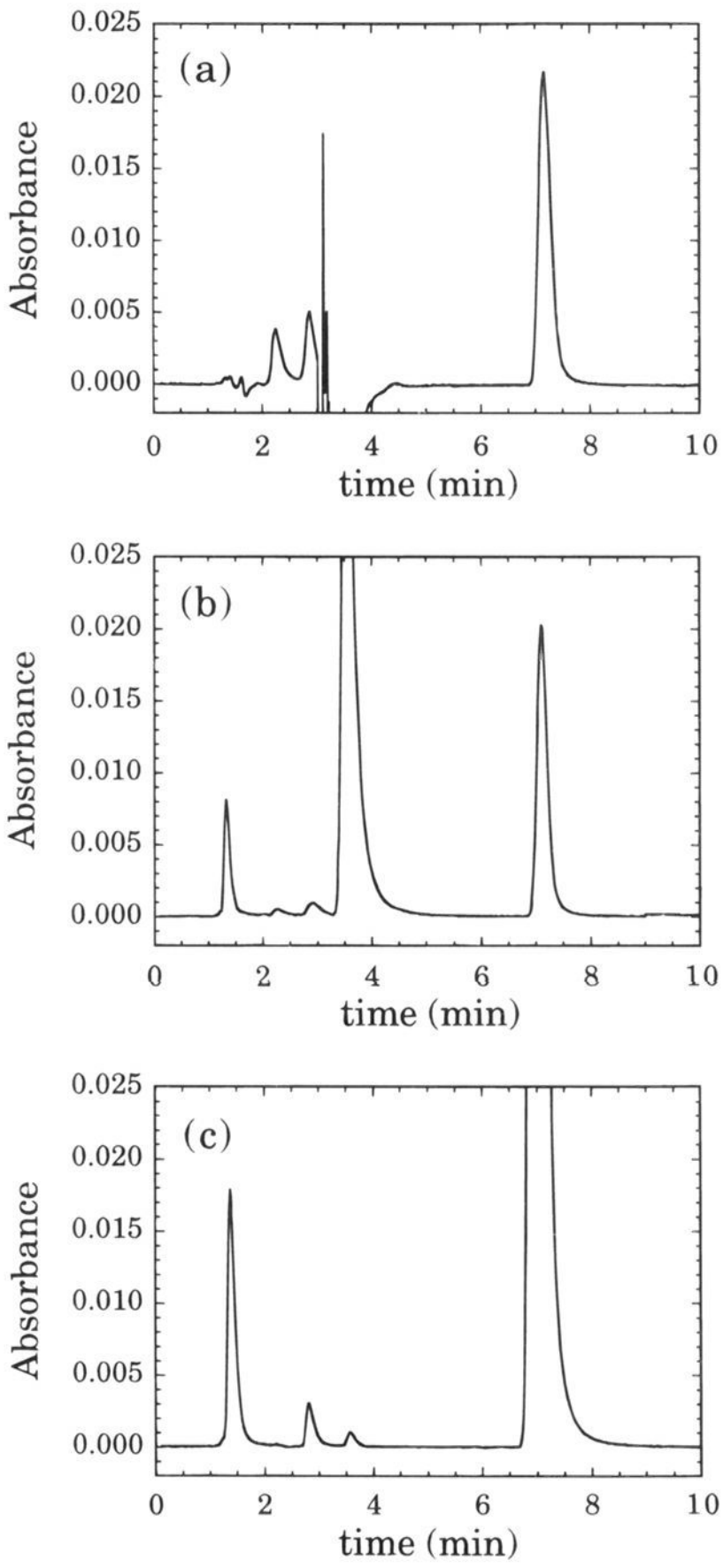

Figure 8. HPLC chromatograms at 266 nm of the reaction of (a) 8 mM TMP and 0.09 mM Ru(tpy)(bpy)O^{2+} 45 min after mixing, (b) 0.1 mM TMP and 0.2 mM Ru(tpy)(bpy)O^{2+} 400 min after mixing, and (c) 0.5 mM thymine and 0.8 mM Ru(tpy)(bpy)O^{2+} 24 h after mixing. The chromatogram in panel a is a subtraction of a TMP blank at the same concentration from the actual data. Inexact subtraction of three small impurity peaks in the 1−2 min range accounts for the noise in the baseline in this range. Overlaying the chromatogram with the blank reveals about a 1-s difference in retention times, which accounts for the incomplete subtraction, but no difference in peak heights, indicating that these impurities do not participate in the reaction. The trace from 3 to 4 min in panel a is in a region where the large excess of TMP absorbs completely, which gives no viable data. The retention times of TMP and T are 3.6 and 7.1 min, respectively.

of this side reaction to the observed reaction products, 0.5 mM thymine was incubated overnight in the presence of 0.8 mM Ru(tpy)(bpy)O^{2+}. The appearance of signals at 1.3 and 2.9 min (Figure 8c) with spectra and retention times identical to those observed in the TMP oxidation reaction suggests that thymine

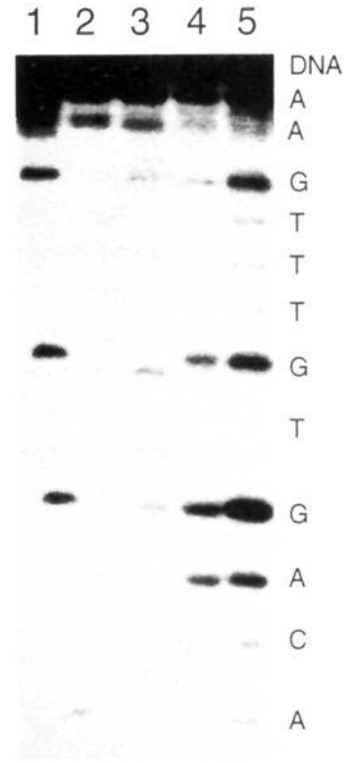

Figure 9. Autoradiogram of a polyacrylamide gel showing the results of the oxidation of 5′-^{32}P-labeled hairpin DNA 5′-TTCAACAGT-GTTTGAA. The reaction conditions were the following: [DNA] = 4 μM (13 000 cpm ^{32}P), [Ru(tpy)(bpy)O^{2+}] = 24 μM, 10 mM sodium phosphate (pH 7.06) at 20 °C. Lane 1, Maxam-Gilbert G+A lane; lane 2, DNA + piperidine treatment (90 °C, 30 min); lane 3, Ru(tpy)(bpy)-O^{2+} + DNA; lane 4, Ru(tpy)(bpy)O^{2+} + DNA with heat only; lane 5, Ru(tpy)(bpy)O^{2+} + DNA with heat and piperidine treatment. All other procedures are as described in ref 7.

oxidation is primarily responsible for the nonquantitative yield of free thymine observed in TMP oxidation.[31]

Efficiencies of DNA vs RNA Cleavage. As stated earlier, there are a number of reports in the literature that suggest that RNA is significantly less reactive than DNA toward metal-based oxidants that effect cleavage via sugar oxidation.[13,14] We have recently observed that Ru(tpy)(bpy)O^{2+} cleaves the mRNA from the iron recognition element (IRE)[32,33] at only a single site in the 80-nucleotide fragment.[34] In order to compare directly the relative reactivities of DNA and RNA, we have performed an analogous oxidation on a synthetic deoxyoligonucleotide based on the 16 nucleotides comprising the hairpin loop of the IRE. In the design of the oligomer d[5′-$T_1T_2C_3A_4A_5C_6A_7G_8$-$T_9G_{10}T_{11}T_{12}T_{13}G_{14}A_{15}A_{16}$], U sites from the IRE[32,33] were replaced with T. As shown in Figure 9, cleavage bands were observed upon oxidation with Ru(tpy)(bpy)O^{2+} at nearly every site in the oligomer. In contrast, only the site analogous to G_8 was cleaved in the IRE mRNA.[34] It therefore appears that Ru(tpy)(bpy)O^{2+} is considerably more reactive toward DNA than RNA, as has been observed with other cleavage agents.[13,14]

Discussion

Oxidation Mechanism. In oxidation of model sugars and mononucleotides, the site of oxidation cannot be regulated by

(31) To search for other reaction products, particularly sugar oxidation products, from the stoichiometric oxidation of TMP by Ru(tpy)(bpy)O^{2+}, chromatograms were measured over a 60 min time range using the buffer/acetonitrile gradient elution. Surprisingly, no other bands were observed in this time range excepting a broad band at ~34 min for [(tpy)(bpy)Ru-$(OH_2)]^{2+}$. The reaction was repeated with 5′-TMP-*p*-nitrophenyl ester, which contains an absorptive tag on the phosphate. The chromatogram of the reaction product showed three new bands, all of which had absorption spectra with λ_{max} between 290 and 310 nm. None of these bands corresponded to *p*-nitrophenol.

(32) Theil, E. C. *Biofactors* **1993**, *4*, 87−93.

(33) Klausner, R. D.; Rouault, T. A.; Harford, J. B. *Cell* **1993**, *72*, 19−28.

(34) McKenzie, R. A.; Lin, P.-N.; Theil, E. C.; Thorp, H. H. Submitted for publication.

the polymer structure, as can occur in studies of natural DNA and RNA. Thus, the extent of oxidation of any particular C−H bond is controlled only by the relative reactivity of each site. We have shown that in natural DNA, oxidation by Ru(tpy)(bpy)O^{2+} occurs from the minor groove at the 1′ position, according to Scheme 1. This conclusion is based on the observations of phosphate termini in both 5′- and 3′-labeled oligomers, modified termini in 5′-labeled oligomers, the furanone product **4**, and distamycin competition.[7] Abstraction of the 1′, 4′, and 5′ hydrogens has been observed for small molecules that bind in the minor groove, so selection of the 1′ position by Ru(tpy)(bpy)O^{2+} must occur partly because of the innate reactivity of the site. Since the 5′ position is a CH_2 site, it is likely to be more difficult to oxidize. In fact, recent theoretical studies have suggested that the C−H bond strengths at the 1′, 3′, and 4′ positions in deoxyribose are significantly lower than for the 2′ and 5′ positions with the 1′ position slightly lower than for 3′ and 4′.[35] If the nucleic acid base is more electron releasing than hydroxyl, the 1′ position may become significantly more reactive in nucleotides compared to deoxyribose.

Several observations in the product analyses argue for the sugar oxidation pathway occurring primarily at the 1′ position in the model nucleotides. We have detected the nucleic acid bases as the main product in the oxidations of the A, T, and C nucleotides. For CMP, we observe a quantitative yield of cytosine based on the loss of CMP, and for TMP, we have observed an 80% yield of thymine based on the amount of Ru(tpy)(bpy)O^{2+} consumed. Under conditions of excess Ru(tpy)(bpy)O^{2+}, the reduced yield (60%) of thymine based on TMP consumed can be ascribed to additional pathways involving base oxidation and not oxidation at an additional site in the sugar. Oxidation at the 3′ or 4′ positions would be expected to produce either base propenoic acid or base propenal, respectively, and we have not detected either of these products under conditions where both are readily detected.[36,37]

The kinetic studies also argue strongly for 1′ oxidation. First, all of the nucleotides are more reactive than deoxyribose and ribose. This result can be ascribed to more effective activation of the 1′ position by the nucleic acid base compared to hydroxyl, which is likely to be less electron donating. This trend is evident even after correction of the rates for the electrostatic binding preequilibrium. In fact, this same trend is evident in similar rate constants for oxidation by the excited state of $Pt_2(pop)_4^{4-}$.[38] Since $Pt_2(pop)_4^{4-}$ is a tetraanion, the reactions of nucleotides are actually discouraged electrostatically relative to the neutral sugars, yet nucleotides are more reactive by about an order of magnitude in rate constant. Second, the lower reactivity of the 2′-oxy nucleotides and sugars toward Ru(tpy)(bpy)O^{2+} can be ascribed to deactivation of the 1′-position by the 2′-hydroxyl,[18] which also argues primarily for oxidation at the 1′ position. This observation has also been made for quenching of $Pt_2(pop)_4^{4-}$ (Table 3).[38]

Relative Reactivity of DNA and RNA. The difference in rate constants for oxidation of deoxy and oxy substrates is intriguing from the point of view of understanding why many cleavage agents produce far fewer scissions in RNA compared to DNA. For example, Holmes and Hecht have observed that FeBLM cleaves a tRNA and its tDNA analogue at the same singular site at low concentration.[13] Upon raising the concentration of FeBLM, new non-specific sites appear for tDNA but not for tRNA. Lim and Barton have also observed far fewer cleavage sites in $tRNA^{phe}$ compared to the tDNA analogue.[14] A generally lower reactivity for RNA compared to DNA also has been observed for Fe(EDTA)$^{2-}$ and copper-phenanthroline,[39,40] although no direct DNA and RNA analogues have been compared. We have observed that the 80-nucleotide mRNA from the iron recognition element is cleaved at only a single site by Ru(tpy)(bpy)O^{2+}.[34] As shown in Figure 9, the analogous DNA 16-mer corresponding to the hairpin loop is cleaved at numerous sites by our reagent. Thus, it appears that DNA polymers are also considerably more reactive than RNA polymers toward Ru(tpy)(bpy)O^{2+}, as with the other reagents mentioned above.

Table 3. Ratio of the Rate Constant of Oxidation of 2′-Deoxy Forms to the Rate Constant for Oxidation of the 2′-Oxy Forms of Sugars and Nucleotides

substrate	Ru(tpy)(bpy)O^{2+} [a]	$[Pt_2(pop)_4]^{4-}$ * [b]
ribose	2.8	6.6
cytidine	5.9	not determined
adenosine	6.4	36

[a] Ratio of k_{deoxy}/k_{oxy} taken from Tables 1 and 2. [b] Ratio of Stern−Volmer quenching rate constants from ref 38.

Scheme 2

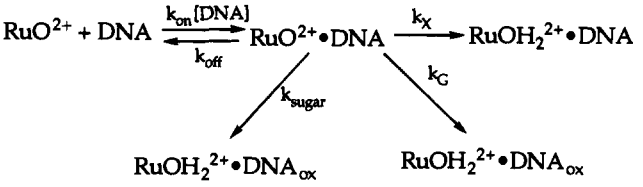

We suggest here that the lower reactivity of RNA compared to DNA toward oxidative chemical nucleases may arise from deactivation of the sugar toward oxidation by the polar effect of the 2′-hydroxyl. This effect would be expected for nucleases that cleave by oxidation at the 1′ position, such as Ru(tpy)(bpy)O^{2+} and Cu-phen.[7,39] While FeBLM activates the 4′ position in DNA,[36,41] Hecht et al. have shown that the 1′ position is oxidized in sugars containing the 2′-hydroxyl group,[42] which could be a major pathway for RNA scission. Thus, this effect could apply to RNA scission by FeBLM as well. The complexes $Rh(phen)_2(phi)^{3+}$ have been shown to target the 3′ position in double-stranded DNA,[37] and while this position is not necessarily the target in RNA, the 2′-hydroxyl might also be expected to deactivate the 3′ position in the same manner as for the 1′ position. Thus, deactivation of the adjacent positions by the polar effect of the 2′-hydroxyl apparently does account for the lower reactivity of RNA toward Ru(tpy)(bpy)O^{2+} and could well account for this same phenomenon in other systems. In addition, these considerations could be important in other biological problems where the relative reactivities of nucleotide radicals play a role in mechanism, as in the ribonucleotide reductases.[43,44]

Relationship to Site-Specific Cleavage Yields. The cleavage of DNA can be analyzed in terms of the mechanism shown in Scheme 2. In this model, Ru(tpy)(bpy)O^{2+} binds to DNA and can then be reduced either via cleavage of DNA by sugar oxidation (k_{sugar}), cleavage of DNA by guanine oxidation (k_G),

(35) Miaskiewicz, K.; Osman, R. *J. Am. Chem. Soc.* **1994**, *116*, 232−238.
(36) Sugiyama, H.; Xu, C.; Murugesan, N.; Hecht, S. M.; van der Marel, G. A.; van Boom, J. H. *Biochemistry* **1988**, *27*, 58.
(37) Sitlani, A.; Long, E. C.; Pyle, A. M.; Barton, J. K. *J. Am. Chem. Soc.* **1992**, *114*, 2303.
(38) Kalsbeck, W. A.; Gingell, D. M.; Malinsky, J. E.; Thorp, H. H. *Inorg. Chem.* **1994**, *33*, 3313−3316.
(39) Sigman, D. S. *Acc. Chem. Res.* **1986**, *19*, 180.
(40) Celander, D. W.; Cech, T. R. *Science* **1991**, *251*, 401.
(41) Stubbe, J.; Kozarich, J. W. *Chem. Rev.* **1987**, *87*, 1107.
(42) Duff, R. J.; de Vroom, E.; Geluk, A.; Hecht, S. M.; van der Marel, G. A.; van Boom, J. H. *J. Am. Chem. Soc.* **1993**, *115*, 3350.
(43) Stubbe, J. *Adv. Enzymol. Relat. Areas Mol. Biol.* **1989**, *63*, 349.
(44) Stubbe, J. *J. Biol. Chem.* **1990**, *265*, 5329−5332.

or self-inactivation (k_X), in which the metal is reduced but DNA is not damaged. In single-stranded DNA, about 20% of the metal complex is reduced via k_{sugar} and about 30% via k_G.[7] The k_X pathway involves the self-oxidation of the oxidant, and we have shown for an $Os^{IV}O^{2+}$ analogue that DNA catalyzes this pathway by increasing the effective concentration of the oxidant through binding. Consistent with this idea is the observation here of an 80% yield based on $Ru^{IV}O^{2+}$ for the oxidation of TMP to T. Comparison of this yield to a 50% yield of total oxidation in DNA suggests that k_X is better able to compete with substrate oxidation in polymeric DNA compared to the mononucleotides, again supporting the idea that condensation of the metal complex on the polymer leads to an increased k_X.

From densitometry of sequencing gels, we have observed previously that the ratio of cleavage at G to cleavage at any of the other nucleotides is about 7:1 on a per nucleotide basis, i.e. $k_G/k_{sugar} = 7$.[7,45] This ratio was obtained in single-stranded DNA where we would expect very little control of the cleavage pattern by the oligomer structure, and the reactivity should largely control the extent of cleavage at each site. From the data in Tables 1 and 2, we can calculate an average k_{sugar} for TMP, dCMP, and dAMP of 1.2 M^{-1} s^{-1}. Using the value of $k_G = 9$ M^{-1} s^{-1} obtained from the analysis in Figure 6, *the ratio calculated from the kinetic data is $k_G/k_{sugar} = 7.5$, which is in excellent agreement with the ratio calculated from densitometry of sequencing gels of single-stranded DNA.* Thus, we can make predictions about the cleavage pattern based on the kinetic studies. In future experiments, we will be able to understand when the DNA structure is in control of the cleavage pattern by understanding when the cleavage ratios do not match with the kinetic data on the mononucleotides.

(45) We have shown that guanine bases are released from DNA oxidations,[10] and we have observed modified phosphates at guanine sites in sequencing gels prior to piperidine treatment.[7] Thus, cleavage at guanine results from both guanine oxidation and sugar oxidation. The yield of released guanine is similar to that of adenine, thymine, and cytosine, so in analyzing cleavage patterns to obtain the relative rate constants for guanine and sugar oxidation, we have made the assumption that the extent of sugar oxidation at all four nucleotides is about the same.[7] However, here we are comparing the rate of *total* oxidation at G to oxidation at A, T, and C. In GMP, the observed rate k_1 does contain a contribution from both sugar and base oxidation, although the base contribution is clearly much larger, especially since GMP contains a ribo sugar, which is less reactive.

Another important point here is that the oxidant apparently oxidizes the same site in mononucleotides and DNA. This observation suggests that the 1′ site is the most reactive site in the sugar and that the oxidant discriminates on the basis of reactivity. This idea is consistent with the much lower oxidation potential of Ru(tpy)(bpy)O^{2+} (0.6 V) compared to more reactive species such as high-valent oxoiron functionalities,[41,46] high-valent copper species,[39] or UV excited states of coordinated ligands.[37] Accordingly, FeBLM and copper phenanthroline have both been shown to activate both the 1′ and 4′ hydrogens under appropriate conditions,[36,39,41,42] while Ru(tpy)(bpy)O^{2+} is apparently competent only to oxidize the 1′ position. Controlling the selectivity of Ru(tpy)(bpy)O^{2+} by tuning the redox potential of the oxidant is therefore fruitful,[11] whereas minor changes in the driving force for more reactive cleavage agents are not likely to alter the cleavage pattern.

Conclusions

We have shown that Ru(tpy)(bpy)O^{2+} oxidizes model nucleotides and sugars with varying efficiencies. The product analyses and trends in rate constants support oxidation at the 1′ position, as has been seen for natural DNA.[7] It is possible to make a number of useful comparisons between the model rate data and the cleavage pattern in polymeric nucleic acids. First, the rate constants are significantly lower for 2′-oxynucleotides compared to deoxynucleotides, which probably arises from destabilization of the 1′ carbocation (or radical) by the polar effect of the 2′-hydroxyl.[18] As predicted from this observation, considerably fewer cleavage sites are observed for RNA compared to analogous DNA oligomers. Second, the yield of oxidation products is considerably higher based on $Ru^{IV}O^{2+}$ for the model nucleotides (80%) than for DNA (50%), which is consistent with our recent demonstration that DNA catalyzes the self-inactivation of the oxidant.[7] Finally, the ratio k_G/k_{sugar} determined from the kinetic data is the same as that determined by densitometry of DNA sequencing gels.

JA943369V

(46) Hecht, S. M. *Acc. Chem. Res.* **1986**, *19*, 83.